Coronal Cavity Magnetic Fields Inferred by DKIST/CryoNIRSP

Elizabeth Wraback[1], Samaiyah Farid[2], Thomas Schad[3], Urszula Bąk-Stęślicka[4], Giuliana de Toma[1], Yuhong Fan[1], Sarah Gibson[1], Mari Paz Miralles[5], Jie Zhang[6], Suman Dhakal[6]

[1]High-Altitude Observatory, National Center for Atmospheric Research, [2]Alabama A&M University, [3]National Solar Observatory, [4]University of Wrocław, [5]Center for Astrophysics | Havard & Smithsonian, [6]George Mason University

ewraback@ucar.edu

1. Introduction

Coronal Cavities as CME Pre-Cursors

- Often observed as the **dominant sub-structure in CMEs**, as the dark region surrounding the bright core (Illing & Hundhausen 1986, Gibson et al. 2006, Karna & Miralles 2025)
- CoMP/UCoMP linear polarization fraction measurements show a consistent "lagomorph" or V-shape structure in cavities, which **suggests a flux rope pre-eruptive structure**
- In LOS magnetic field measurements of cavities, if we observe O-type or X-type nulls, it could **help discriminate between CME initiation mechanisms** (Gibson et al. 2023)

Goal: infer the LOS magnetic field and structure in a coronal cavity from DKIST/CryoNIRSP observations

2. Context and Observations

We will focus on two cavities, **August 08, 2025** on the NW limb at $\langle X, Y\rangle = \langle 634'', 607''\rangle$ and **October 05, 2025** on the SW limb $\langle X, Y\rangle = \langle 689'', -656''\rangle$.

SDO/AIA 193 Å context image with a normalizing radial gradient filter applied (first column) and 304 Å (second column) for the 08 August 2025 (top row) and 05 October 2025 (bottom row) prominence-cavity systems. The DKIST FOV (blue and green boxes) with the DKIST slit orientation (black line) are shown. The first column includes egg fits to the cavity, where the blue dashed line is the outer boundary, the black dashed line is the dark, low-density cavity, and the red dashed line outlines the horn. The third column contains SDO/AIA 304 Å Carrington maps of CR 2300 (top) and 2302 (bottom), created based on the limb plotting method of Karna et al. (2015). We include the DKIST pointing projected onto the map as the red cross, highlighted by the red box.

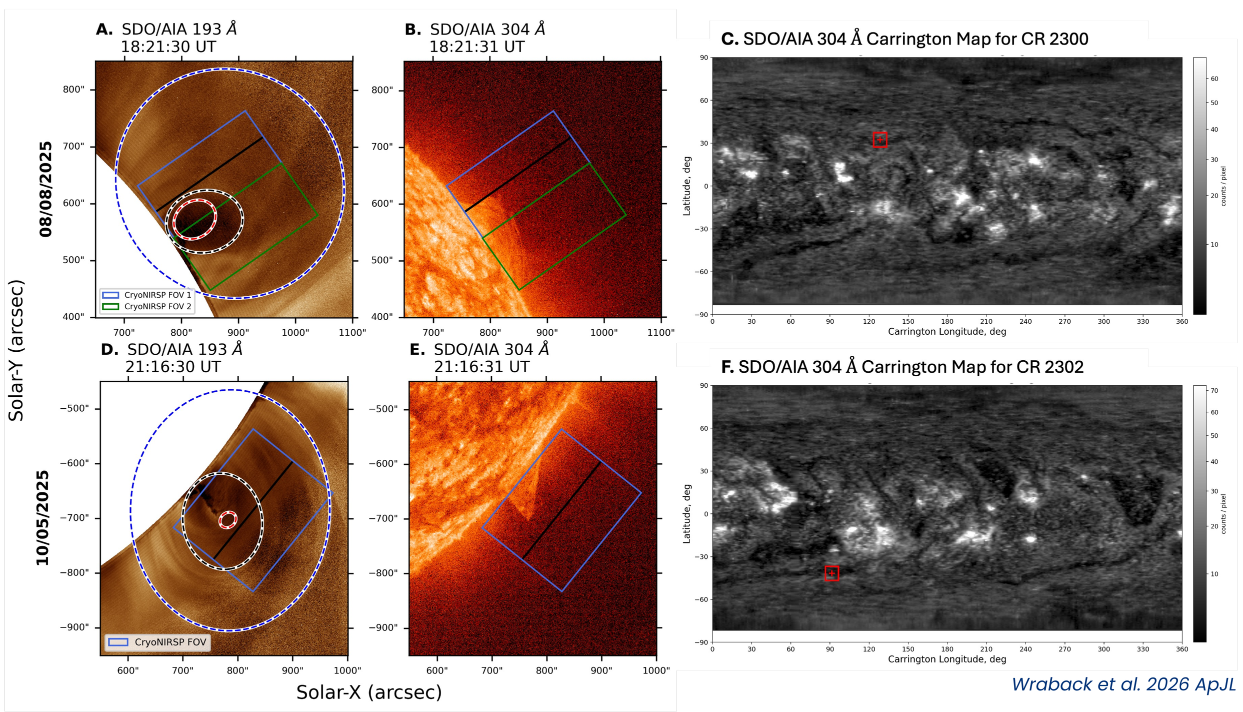

DKIST CryoNIRSP Observations

The **August 08, 2025 observation** consists of two raster maps created with a radially-oriented slit that sequentially mapped a contiguous region centered at $\langle X, Y\rangle = \langle 880'', 605''\rangle$ with a combined FOV of $224'' \times 460''$. Each map had 241 steps ($0''.5$ step width) and two repeated measurements resulting in 11.6 s of cumulative integration time.

The **October 05, 2025 observation** consists of a 101-step ($1''.84$ step width) raster map with the slit oriented parallel to the limb, where each measurement was repeated 12 times, resulting in a cumulative integration time of 69.6 s. The map is centered at $\langle X, Y\rangle = \langle 847'', -683''\rangle$ with a FOV of $188'' \times 231''$.

3. Results from Fitting Stokes I, Q, and U

Spectropolarimetric observations of the Fe XIII 10747 Å forbidden emission line, including the coronal line peak amplitude, Doppler velocity, line width, and linear polarization fraction (L/I) (from left to right) for the 08 August 2025 (top row) and 05 October 2025 (bottom row) cavities. The linear polarization angle is shown as the pink lines plotted over the linear polarization fraction. The egg fits to the cavities are included for context. For the 05 October 2025 cavity, we outline the prominence in green, based on the continuum signal in the Fe XIII observation.

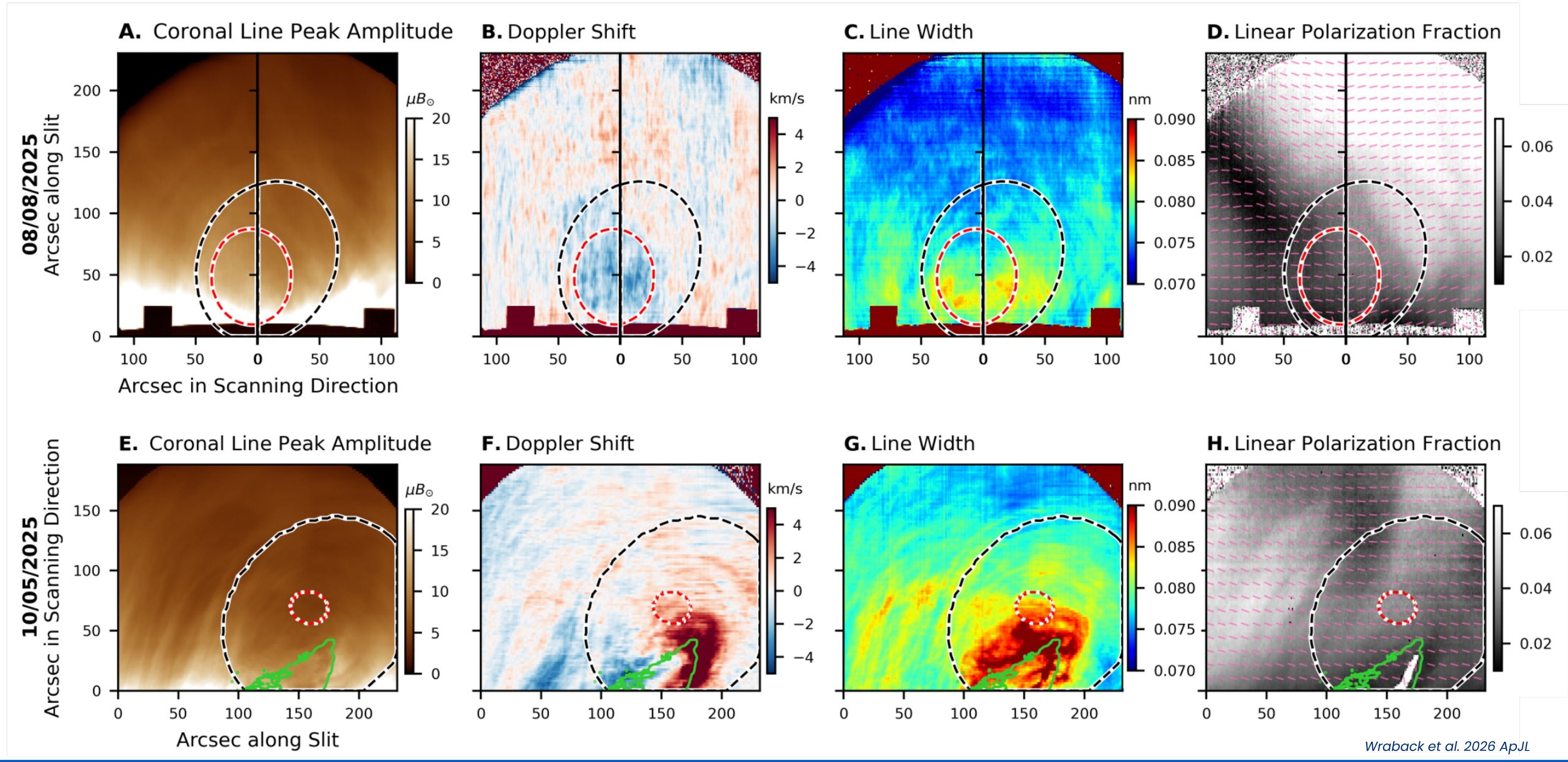

4. Stokes V and BLOS

Left: Estimated LOS magnetic field in the 08 August 2025 (top row) and 05 October 2025 (bottom row) cavities and their embedded prominences, masked to **show only 3σ significant observations** (first column). The second column shows the signed red-wing amplitude of the antisymmetric Stokes V profile. Each plot shows the egg fits to the cavity, for context. For the 05 October 2025 cavity, we outline the prominence in green based on the continuum signal in the Fe XIII observation.

Right: Corrected Stokes I, Q, U, and V (panels A-D) along the slit at one step along the scanning direction (purple) and the fit to the observations (red; panels E-H) at a single location on the slit (cyan).

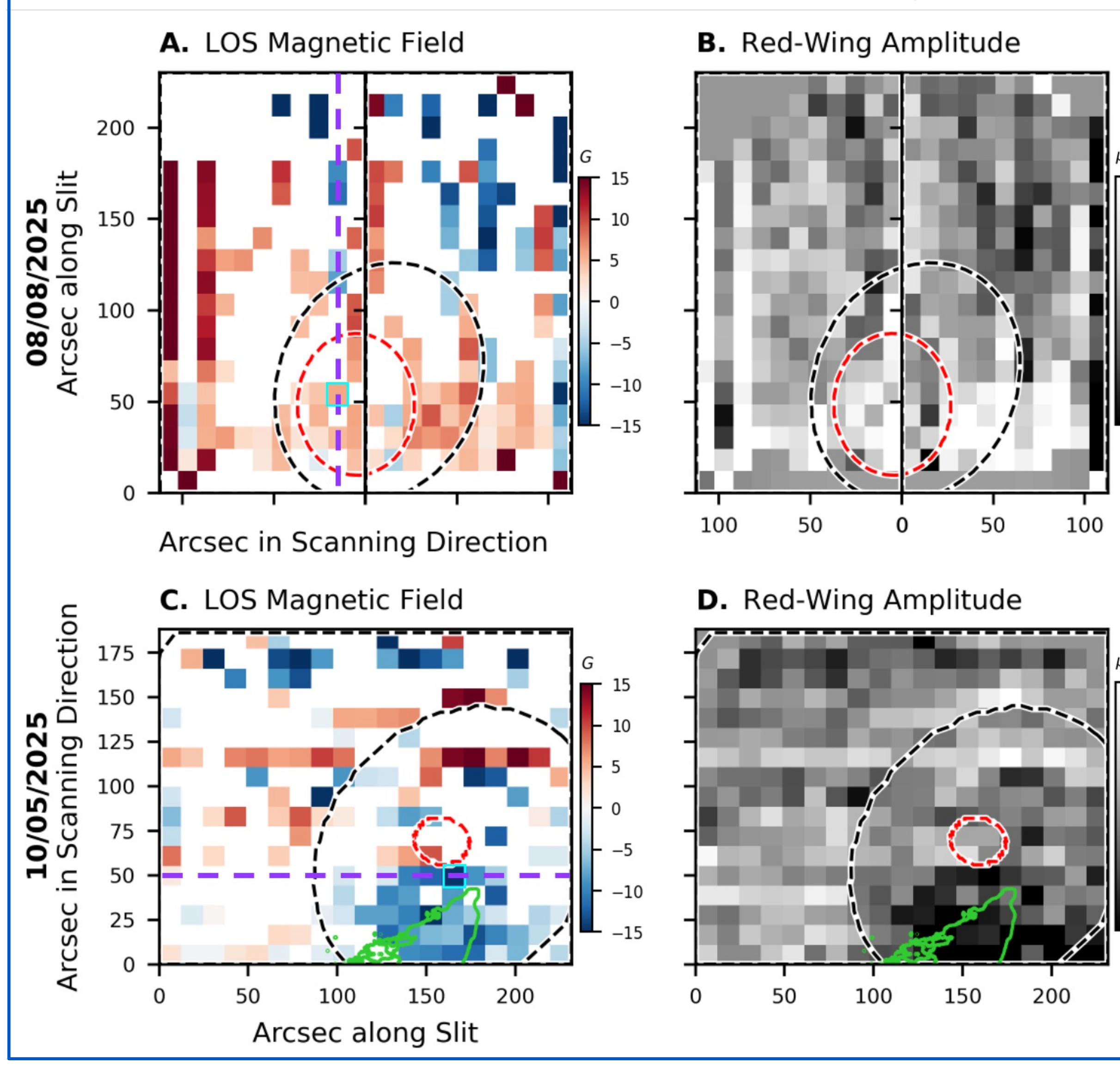

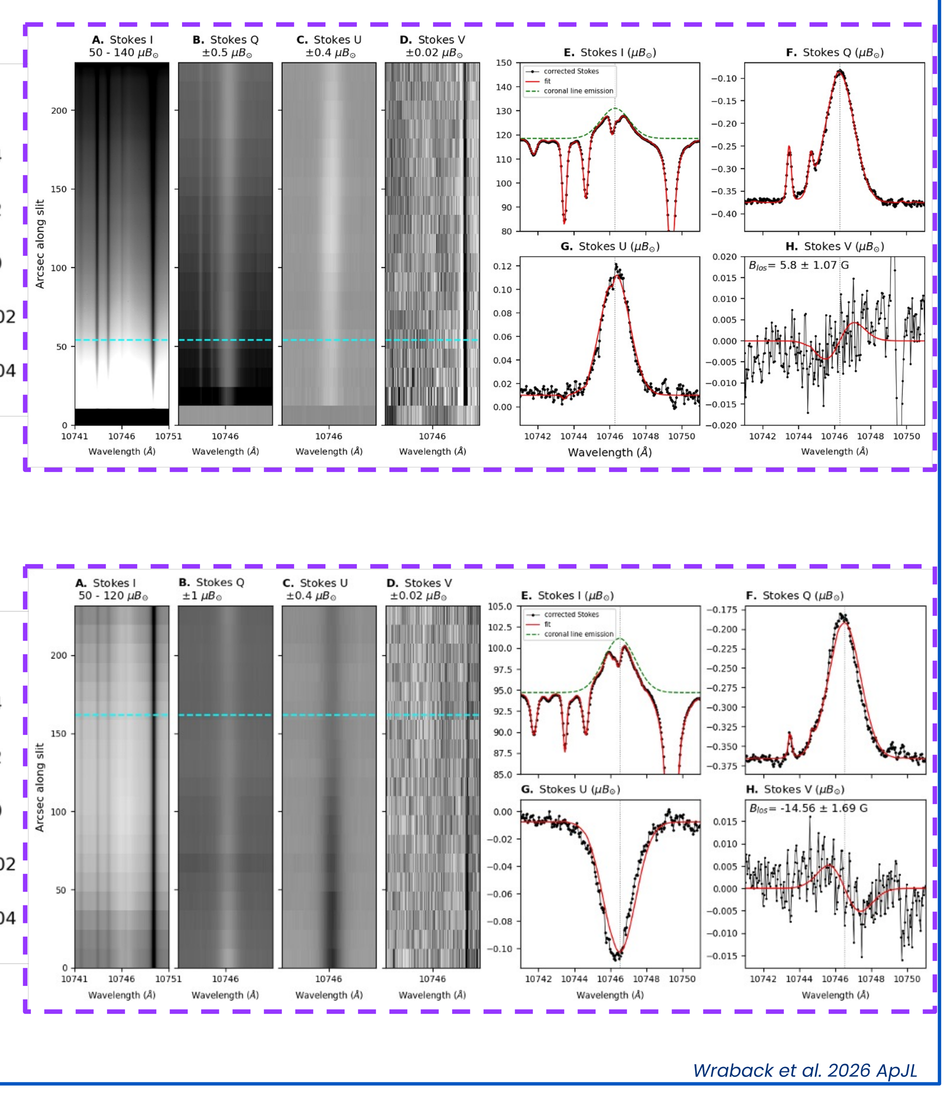

5. Why can't we observe BLOS everywhere in the cavity?

Noise: preliminary modeling results (modified from Fan & Liu 2019) suggest that at this noise level for this observation scheme, we should only observe BLOS in the around the prominence and in the horn

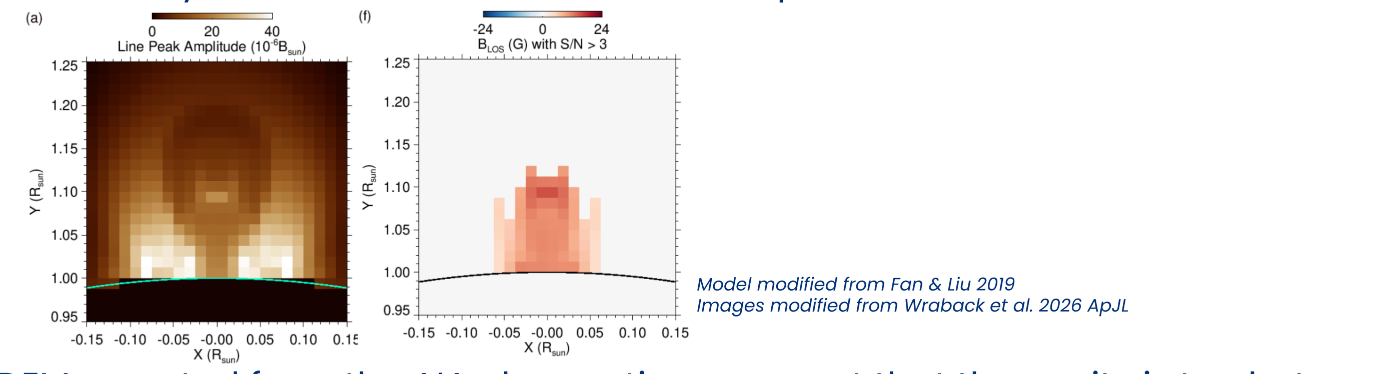

Temperature Structure: DEMs created from the AIA observations suggest that the cavity is too hot (~2.3 MK) in comparison to the formation temperature of Fe XIII (~1.6 MK)

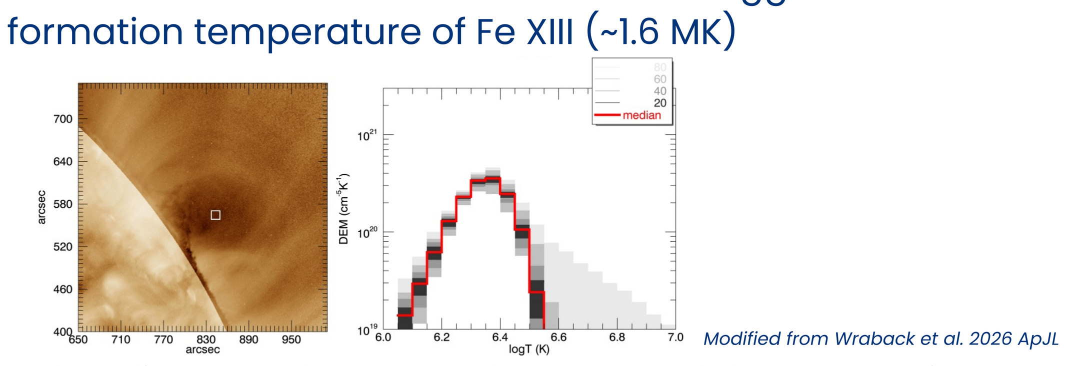

Geometric effects: how does the alignment between observer and the magnetic structure in the cavity effect how we are measuring Stokes V? *Current work!*

6. Implications for COSMO

Large Coronagraph (LC) in the Coronal Solar Magnetism Observatory (COSMO)

- COSMO/LC is a ~1.5 m refractive telescope that would provide daily spectropolarimetric observations of the global solar corona out to 2.5 $R_\odot$ in visible and near-IR wavelengths
- **Despite the relatively low density in a cavity, they are viable targets for COSMO to *routinely* measure the magnetic field in the corona because of their intrinsic LOS alignment**
- Challenges with DKIST include:
  1. the restricted FOV that can be scanned in a reasonable observing time (~hours) to obtain a detectable Stokes V signal → we only have 6 unique cavity observations
  2. background of ~100 ppm
- COSMO's solutions:
  1. large FOV and the synoptic mode of operations, which will enable detection and analysis of a large number of cavities
  2. use a lens rather than a mirror to reduce stray (Gallagher et al. 2016) for an expected background of ~5 ppm

This material is based upon work supported by the NSF National Center for Atmospheric Research, which is a major facility sponsored by the U.S. National Science Foundation under Cooperative Agreement No. 1852977. Any opinions, findings and conclusions or recommendations expressed in this material do not necessarily reflect the views of NSF.